

# Chapter 1

## Summary

The interface between air and ice governs many phenomena that are essential to chemical processes in the atmosphere. Ice ever-present in the atmosphere and possess a wide range of microenvironments in which trace gases can interact, including a quasi-liquid disordered layer (Toubin et al., 2001; Bartels-Rausch et al., 2014). Studies connected to ice indicate that it can initiate and influence photochemical processes that could lead to ozone destruction (Solomon, 1999; Abbatt, 2003) in the troposphere. In view of this, chemical processes at the air/liquid interface have attracted a lot of scientific research, of particular interest is acids with liquid water or water-like layer on ice. A number of surface sensitive techniques including Infrared spectroscopy (Darvas et al., 2012) and vibrational sum frequency spectroscopy (Gordon et al., 2018) have been conducted over the years to derive information about the electronic properties of such reaction through the study of the hydrogen-bonding and proton transfer of such reaction. The reason being that the dissociation of trace gases upon interaction with liquid water or the liquid-like layer on ice surface is related to the distortion of the hydrogen-bonding network. X-ray photoelectron spectroscopy (XPS) is one of the most well-established methods to provide detailed information about the chemical composition and electronic properties of molecular systems (Hüfner, 2013) given its surface sensitivity. XPS has been applied to investigate the properties of various molecules at the core-valence region. Studies at interface between metal oxides such as Bismuth Vanadate (Starr et al., 2017), Magnesium oxide (Newberg et al., 2011), and  $\alpha - Fe_2O_3$  (Yamamoto et al., 2010) and

aqueous electrolyte solution have indicated that XPS is a powerful tool to investigate the binding energies at the core-valence region. These studies revealed that XPS is able to resolve metal oxide, hydroxyl, surface molecular water and water vapor peaks arising from the core-valence region of water adsorption on metal surface based on their binding energies. Studies into the adiabatic electron binding energies of gaseous species including Uraniumpentachloride (Su et al., 2013) and Uranyl tetrafluoride (Dau et al., 2012) indicate that XPS suitable to study ionic bonding of heavier halogen complexes at the core-valence level. Studies conducted by (Olivieri et al., 2016) with XPS to investigate the ionization energies of aqueous solutions at the core level revealed huge shift in ionization energies of gas phase water in the presence of liquid water and that the ionization energy of the liquid water depends on the chemical composition of the solution. Quite recently, the use of XPS to study the surface of saturated sodium chloride (Tissot et al., 2015; Gaiduk et al., 2016) indicate that XPS is able to resolve ionic chlorine form aqueous solution of sodium chloride based on the core level shift of binding energies with respect to the bulk liquid. XPS has also been utilized to investigate the impact of acids on liquid water or water ice at the air-liquid interface at core-valence level. Investigations into the bound state of weak acid such as 2-propanol (Newberg and Bluhm, 2015), acetone (Starr et al., 2011) and acetic acid (Krepelova et al., 2013) on ice surface indicate that such species do not produce any significant changes in the hydrogen-bonding network of water ice. It has been suggested that, strong acid on ice surface on the other hand fully dissociate leading to modification in the hydrogen-bonding network of water ice at low temperatures (Parent et al., 2011). Quite recently, experiment on the interaction of HCl at warm ice surface revealed a huge chemical shift in binding energy of 2.2 eV between covalent and ionic form of solvated HCl. The photoelectron spectroscopy experiment further revealed that the ionic form of the HCl perturbs the hydrogen bonding network of the water ice by binding them into solvation (Kong et al., 2017). In this respect, there is the need for molecular dynamics simulation in order to either provide theoretical support or give detailed information on the type of bonding at the core-valence regions to the experimental findings.

to provide accurate ground-state photoelectron spectra, including excitation energies of the

interaction hydrogen chloride on ice surface. This complicated approach give reliable ground-and excited-state properties based on its partitioning of large systems into subsystems and taking the effect of the environment on a subsystem of interest into account. Recent formulation of FDE have shown that FDE still possesses an exact framework that allows the DFT to be substituted with WFT for Theoretical studies based on semi-empirical method aimed to provide understanding of the electronic properties of solvated HCl determined no chemical shift in the binding energies between ionic and covalent chlorine. These observations fact that semi-empirical methods overestimate the proton transfer barrier and underestimate the proton affinity of chloride anions (Arillo-Flores et al., 2007). Recent studies probing the ground-state properties of hydrogen chloride in solvent suggest that classical molecular dynamics models coupled with ab initio calculations need parameterization of some of the core-core functions to provide accurate description of intermolecular interactions due to the difficulties to sample transitions from the molecular form to the contact ion pair form (Wick, 2017). These are indication that classical models parameterized with ab initio calculations are prone to problems of potential transferability and lead to poor description of intermolecular interactions and hydrogen bonding between solute and solvents if some of the electronic interactions are not optimized or parameterized. At the moment, the electronic structure calculations to give predictive quantitative description of the ground-state electronic properties of solute-solvent systems such as solvated hydrogen halides including excitation energies is a full quantum mechanics based on the combination of first principle molecular dynamics density functional theory (DFT) and many-body perturbation theory (MBPT) in the  $G_0W_0$  approximation. According to studies on the ionization potential and electron affinity of solute-solvent system, density functional calculations followed by the  $G_0W_0$  approximation (Gaiduk et al., 2018; Pham et al., 2017; Opalka et al., 2014) yield accurate results in self-energy calculations, however, it lacks the ability to account for the presence of spin-dependence in coulombic interactions, inaccurate in its application to large and complex systems, not self-consistent (Aryasetiawan and Gunnarsson, 1998) and computationally costly. An alternative approach to the  $G_0W_0$  approximation to probe the ground-state electronic properties of solute-solvent systems to derive photoelectron spectra is

the coupled-cluster method. Coupled-cluster formalism at the single and double (triple) (CCSD(T)) levels (Bartlett and Musiał, 2007) on water clusters (Blase et al., 2016) and implementations based on equation-of-motion at coupled-cluster single and double levels (EOM-CCSD) (Musiał et al., 2011) on water clusters (Lange and Berkelbach, 2018) have been applied to probe the ionization potential at the ground-state level. These studies indicate that the use of DFT followed by CC approaches predicts binding energies of solvent systems accurately with small errors compared to  $G_0W_0$ , which underestimate the ionization potential. In addition, prediction of the ionization potential of water clusters based on approximate variant of EOM-CCSD (Dutta et al., 2017, 2018) such as P-EOM-MBPT2 yield results that can be compared to  $G_0W_0$  (Lange and Berkelbach, 2018). Not only have the EOM-CCSD proved to be a significant tool to derive the electronic properties of water clusters but also shown to be a powerful approximation to accurately account for relativistic effects such as spin-orbit coupling in describing the electron affinity, ground- and excited-state properties of halogen species (Shee et al., 2018; Bouchafra et al., 2018). Quite recently, (Peng et al., 2015) have developed a much more elaborate method to target core excitation energies within the EOM-CCSD ansatz based on the core valence separation (CVS) approximation (Cederbaum et al., 1980). This approach is seen to be provide a path that only includes excitations from the essential core orbitals when computing the core-level spectra. In this study, we present the use of a new approach in the DFT in the form the so-called frozen density embedding (FDE) method and CVS-EOM-CCSD one subsystem (WFT-in-DFT) (Gomes et al., 2008; Höfener et al., 2013; Daday et al., 2013) or for all the subsystem under consideration (WFT-in-WFT) (Höfener and Visscher, 2012) as well as the incorporation of coupled-cluster theory, making it possible to calculate the embedding potential for the ground state as well as the excited states at high accuracy and with less computational cost.

In the evaluation of the binding energy of the interaction HCl with ice surface, the statistical averaging orbital potential (SAOP) model (Schipper et al., 2000) would be employed prior to the DFT calculation. Photoelectron spectra obtained with the SAOP model suggest that it provides balanced approach to the exchange correlation potential that predict accurately the ionization en-

ergies (Lemierre et al., 2005; Segala and Chong, 2009) and binding energies of molecules at the core level (Takahata and Chong, 2003). The reason being that, the approximation based on the SAOP model has a perfect long-range (asymptotic) behavior with the ability to reduce self interaction errors in cases where there are discontinuities in the derivative of the total energy as the number of particles varies and also to correctly depict atomic shell structure both in the inner and outer regions which are necessary in the evaluation of ionization potentials in the Kohn-Sham densities(Tecmer et al., 2011) compared to (meta)GGA's, which underestimate the ionization potential in such situation.

## 1.1 Potential Model

To study the adsorption of HCl on ice surface, we describe the surface interaction potential between them. To compute the intramolecular and molecule-surface interaction energy of this system, the charges, center of masses, and radii for each atom and atom pairs were taken and applied to their corresponding force fields. Based on the fact that different force fields employ different parameter sets, the interaction potential arising from the collision between the HCl and the surface of ice was considered as additive, consisting of the sum of pair potentials,  $V_{HCl-H_2O}$  over all water molecules(w), which can be expressed as

$$V_{HCl-ice} = \sum_{w,w_i,j} \frac{q_i q_j}{r_{w_i,j}} + \sum_{w,w_i,j} \frac{C_{6,i,j}}{r_{w_i,j}^6} D(r_{w_i,j}) + \sum_{w,w_i,j} a_{i,j} \exp(-b_{i,j} r_{w_i,j}) \quad (1.1)$$

where the fisrt term on the right hand side of the above equation is the electrostatic potential from the attraction and repulsion between charges of the HCl and water molecules, the second term is the dispersion potential and the last term is the short-range repulsion potential. The  $q_i$ 's and  $q_j$ 's are the charges on the water molecules and the HCl molecule respectively and the  $r_{w_i,j}$  is the distance between the charges. The  $a_{i,j}$  and  $b_{i,j}$  in the repulsion potential contribution are atom-atom parameters (X-Y), where X= H, O and Y= Cl, H . In the case of the dispersion potential, the coefficient  $C_6$  is from  $X - H_2O$ , where i = X, (X= Cl, H) and j =  $H_2O$  based on the Slater-Kirkwood formula, the  $r_{w_i,j}$  is the distance between the centers of mass of the molecules and the  $D(r_{w_i,j})$  is

a damping function.

For the water molecules, point charges based on the TIP4P pair potential model (Jorgensen et al., 1983) was used to describe them. This model type consists of two positive point charges representing the hydrogen atoms (+0.52 au) and a negative point charge (-1.04 au) situated at the bisection of the hydrogen sites near the oxygen atom of the water molecule. For the HCl molecule, it was described with a positive point charge (+0.403 au), a negative point charge (-0.909 au) representing hydrogen atom and chlorine atom respectively and a third positive point charge (+0.506 au) located in a direction opposite the hydrogen atom and 1 au away from the chlorine atom. The values of the parameters  $C_6$  in the dispersion term, and  $a_{i,j}$  and  $b_{i,j}$  in repulsion term to describe the surface interaction potential between HCl on ice were taken from (Woittequand et al., 2007). The value of the  $D(r_{w_i,j})$  was obtained by applying the damping function equation (Kroes and Clary, 1992).

Scalar relativistic (SR) zero-order regular approximation (ZORA) Hamiltonian contain relativistic effects such as spin orbit coupling. It has been shown that, the potential dependent expansion in the ZORA gives a second order differential equation that is variationally stable and is able to provide accurate electron energies and densities of the valence orbitals in self-consistent all-electron and frozen-core calculations (Lenthe et al., 1993).

According to (Van Lenthe and Baerends, 2003), electron basis sets with triple-zeta quality with two polarization (TZ2P) functions added and quadruple-zeta valence quality with four polarization added (QZ4P) can provide accurate orbital energies for chloride anion with reduced error compared to double-zeta (DZ) basis sets. It was suggested that the use of TZ2P and QZ4P in ZORA gives orbital energies that is accurate with less error compared to the use of the fully relativistic Dirac equation.

PBE density functional (Perdew et al., 1996) gives accurate description of the linear response of spin-unpolarized uniform electron gas due its ability to incorporate inhomogeneity effects in the density. In this respect, it is able to predict accurately the correct behavior under uniform scaling, smoother potential potential and atomization of energies of molecules.

Uncontracted augmented triple-zeta basis set with only two correlating d functions is able to describe the spin-orbit splitting of the 2p orbital in chloride at the Dirac-Hartree-Fock level (Dyall, 2016).

## 1.2 Discussion on the potential model

We now discuss the potential energy surface (PES) derived from the classical force fields. At shorter distances for HCl interaction with water molecules on ice, the dispersion potential contribution to the total interaction energy tend to decrease to interatomic distance around 9Å. For the repulsive potential contribution, it increase to around 7Å. In both cases, a constant trajectory is observed for large intermolecular distances at energies around -0.183 eV and 0.00030 eV for the dispersive and repulsive part respectively. The electrostatic potential on the other hand decreased in energy at shorter interatomic distances to a minimum of -0.295 eV around 10Å and then converges to a constant path at larger distances. From figure ??, it can be seen that at large intermolecular distance, the effect of the adsorption on the water molecules on ice is less pronounced and have negligible effect on the total interaction energy due to weak interaction between them. The interaction energy curve derived from the electrostatic as depicted in ?? appears to be similar to the total interaction energy curve in ?. For this reason, we can suggest that the adsorption of HCl on ice surface gives a total interaction energy that evolves mainly from the electrostatic part of the force field and that contribution from the dispersion and repulsion potential play a minor role in the interaction energy of the molecular system of interest.

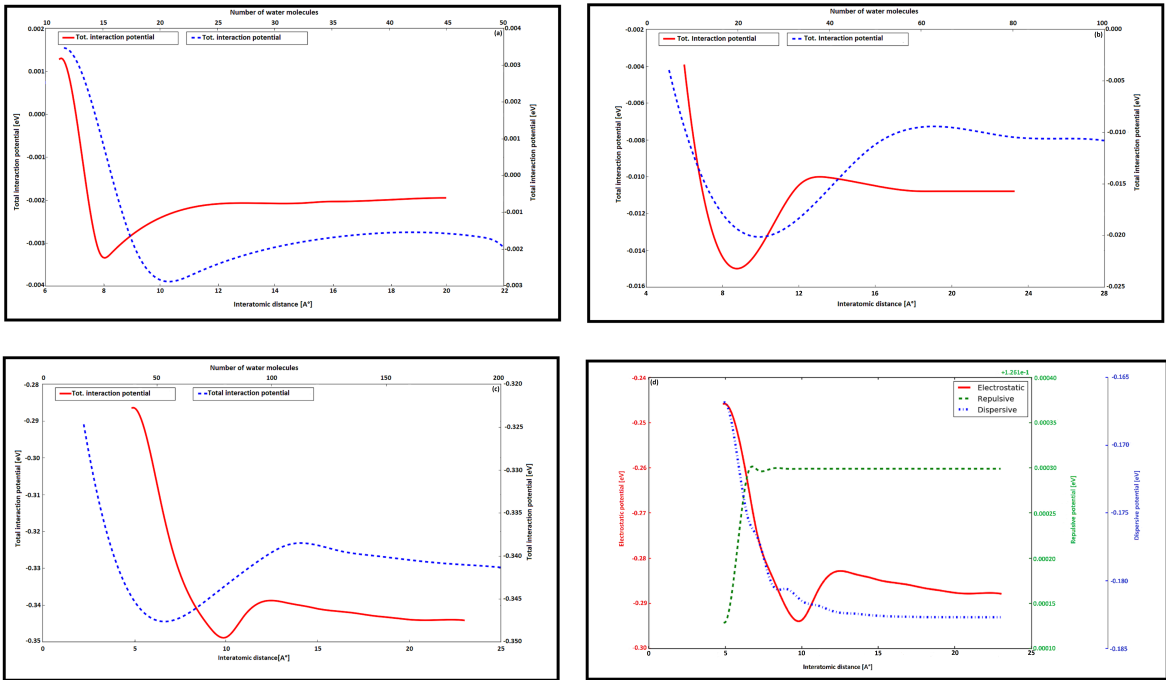


**Figure 1.1:** Variation of the total interaction potential (in eV) for Chloride ion partially solvated in the liquid-like layer on ice surface as a function of water cluster size.

### 1.3 Results of comparison between SAOP and PBE

To evaluate our computational approach, it was essential to compare the effects of water molecules on the halogen of the adsorption of the HCl molecule on ice surface with different functionals. To attain this, we analyzed the orbital energy of our molecular system with the SAOP model and PBE functional. Based on the calculation, it was observed that the GGA's provide inaccurate orbital energy of the highest occupied molecular orbital (HOMO) as the number of water molecules. The PBE functional gave values for the HOMO energy that were either spurious or too high compared to those of the SAOP model as shown in table ???. This attest to the fact that GGA's do not have the right asymptotic behavior to reduce self interaction errors as increase in the number of molecules occurs and can compromise the ionization potential. From figure 1.2, it can be seen the PBE functional has problem with charge transfer due its deficiency to account for integral discontinuity in the total energy for large system. The SAOP model on the other hand proved to be an excellent approximation to compute the HOMO orbital energies and can predict the ionization energy of

the molecular system of interest accurately based on the dependence of the HOMO energy on the ionization potential in the Koopmann's theorem. By comparing both models, we can suggest that the significant number charges allocated to the halogen in the SAOP model and its asymptotic behavior makes the highest occupied molecular orbital (HOMO) more localized and tightly bound compared to the PBE model as the solvent system increases.

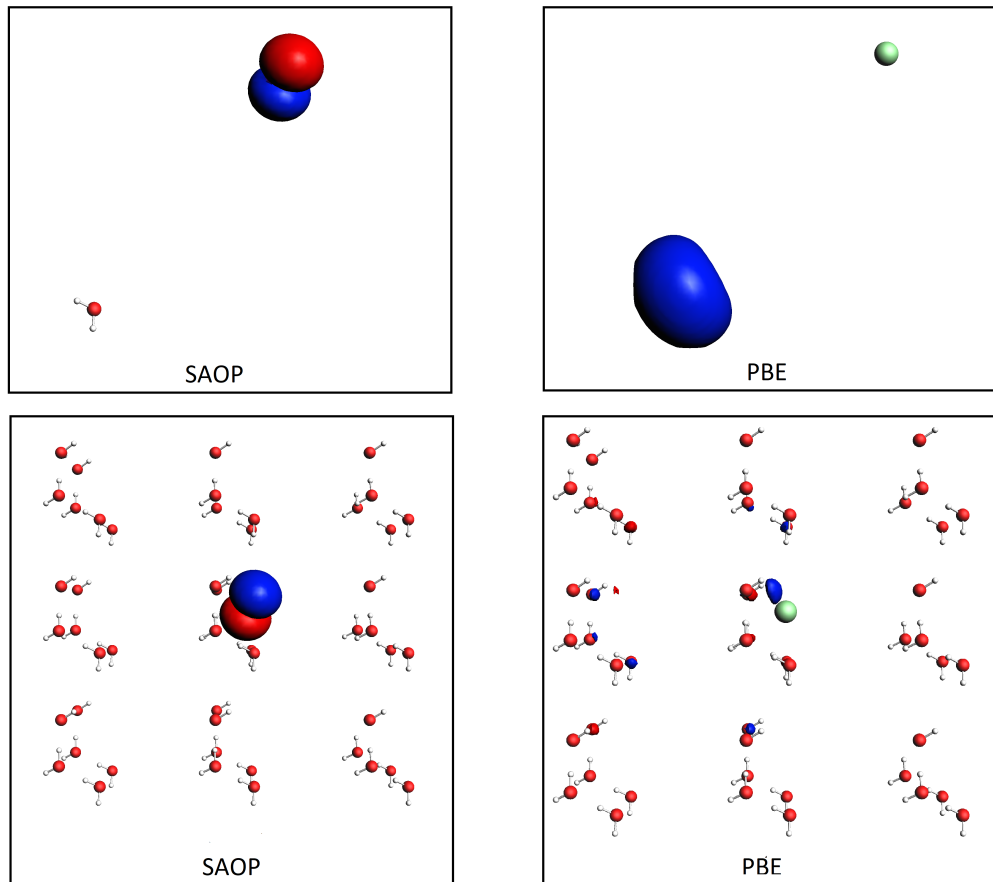


**Figure 1.2:** Localization of the HOMO of solvated chloride ion using different exchange correlation models.

## 1.4 Influence of the water cluster size on the solvated chloride ion: Scalar relativistic effect

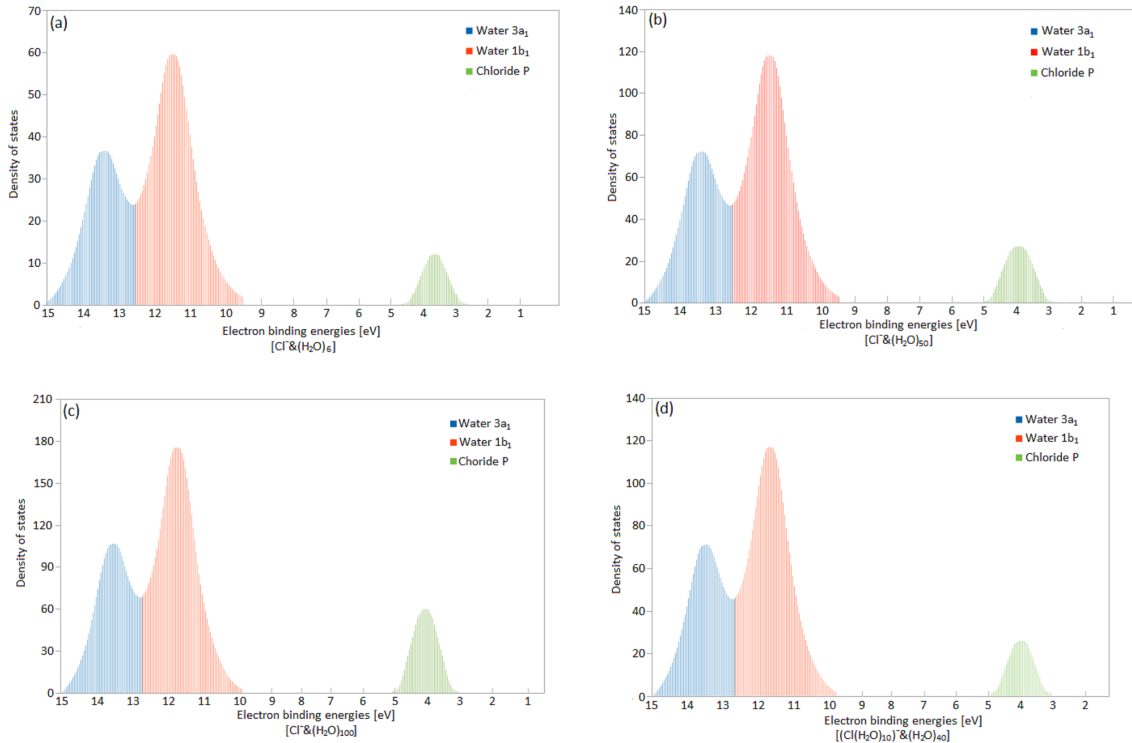


**Figure 1.3:** Average electron binding energies spectra (in eV) for  $[Cl^{-1}/(H_2O)_n]$  and  $[(Cl(H_2O)_{10})^{-1}/(H_2O)_n]$  for various cluster size obtained with SR-ZORA SAOP using quadruple-zeta basis sets

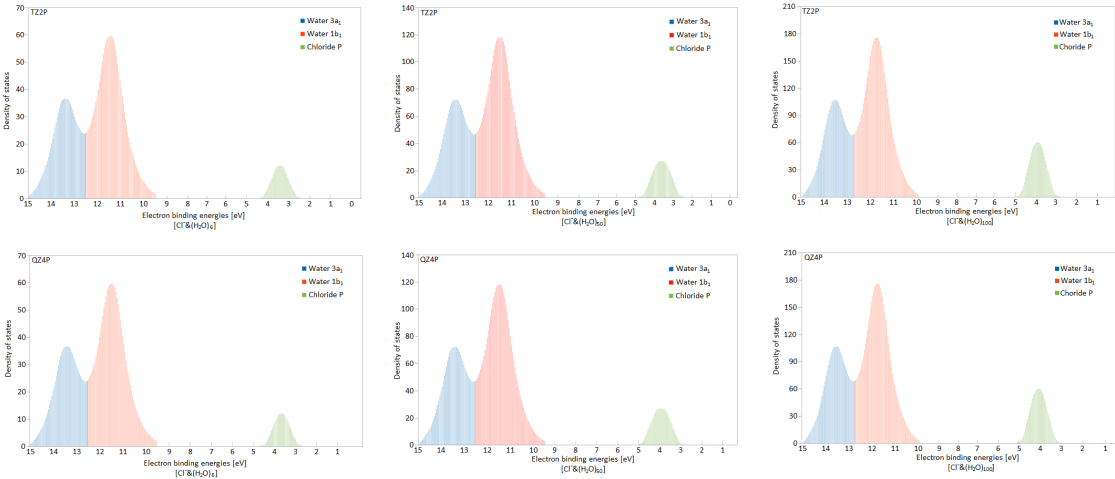


**Figure 1.4:** Average electron binding energies spectra (in eV) for  $[Cl^{-1}/(H_2O)_n]$  for various water cluster size obtained with SR-ZORA SAOP using TZ2P and QZ4P

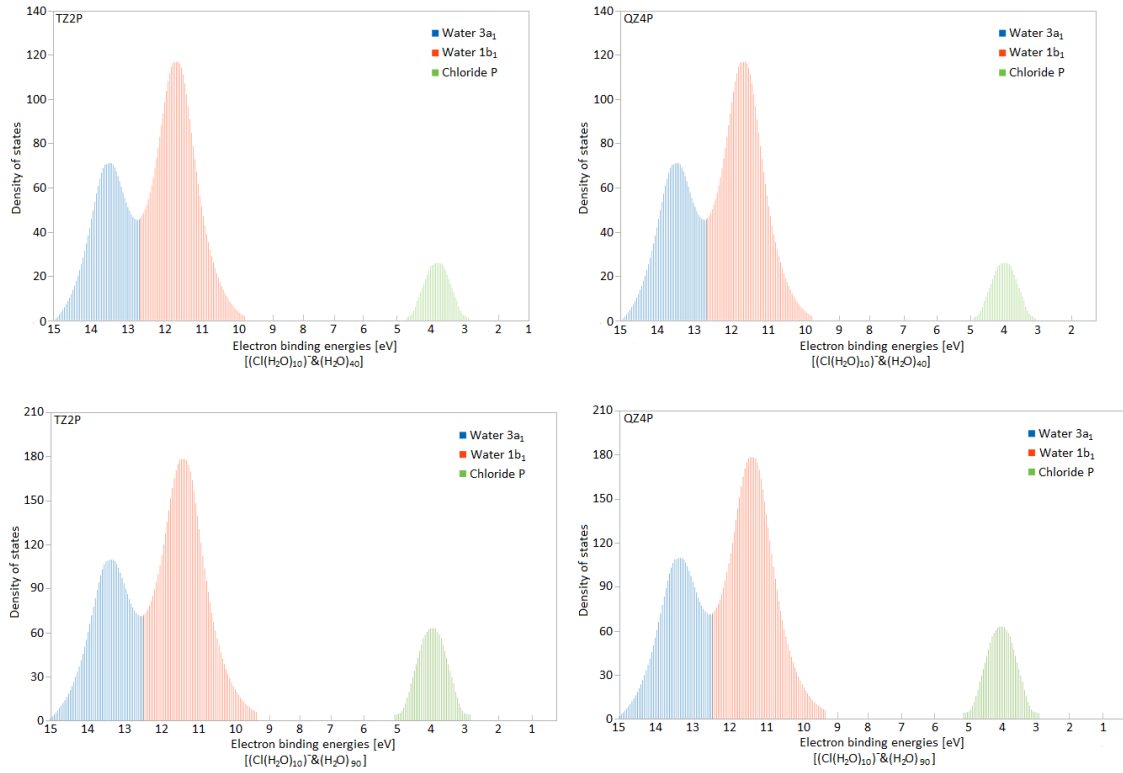


**Figure 1.5:** Average electron binding energies spectra (in eV) for  $[(Cl(H_2O)_{10})^{-1}/(H_2O)_n]$  for various cluster size using the SR-ZORA SAOP using TZ2P and QZ4P

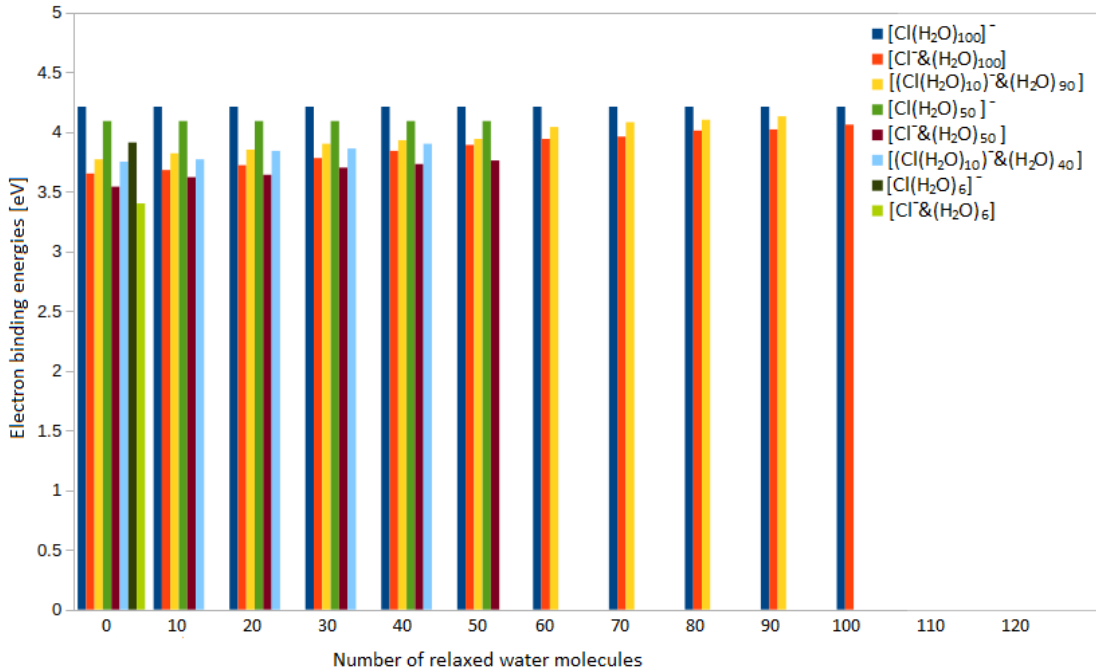


**Figure 1.6:** Variation of the binding energies (in eV) for partially solvated chloride ion for different water cluster size on ice surface with respect to the number of water molecules relaxed in the cluster using the SR-ZORA SAOP in the DFT-in-DFT approach

## 1.5 Influence of the water cluster size on the solvated chloride ion: Effect of Spin-Orbit Coupling

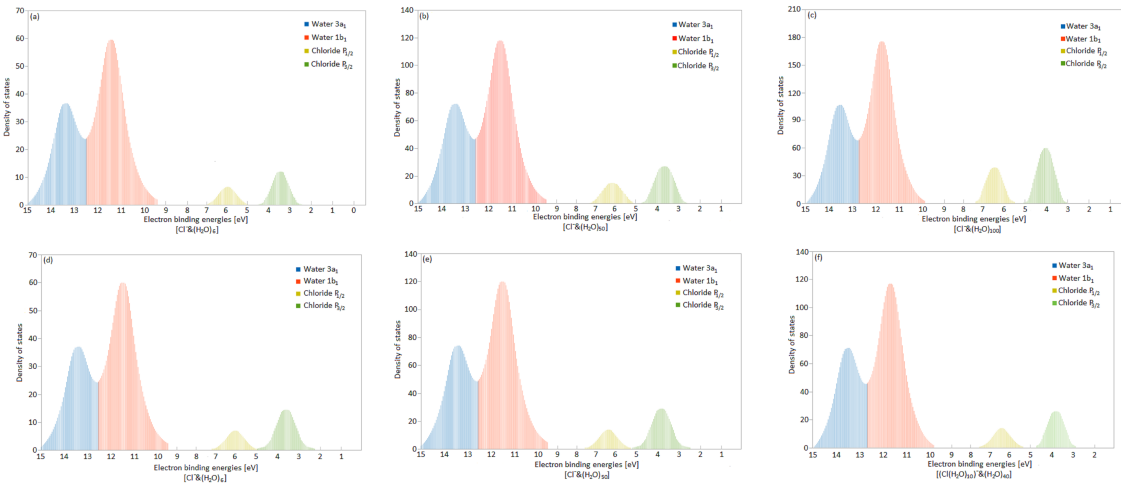


**Figure 1.7:** Average electron binding energies spectra (in eV) for  $[Cl^{-1}/(H_2O)_n]$  and  $[(Cl(H_2O)_{10})^{-1}/(H_2O)_n]$

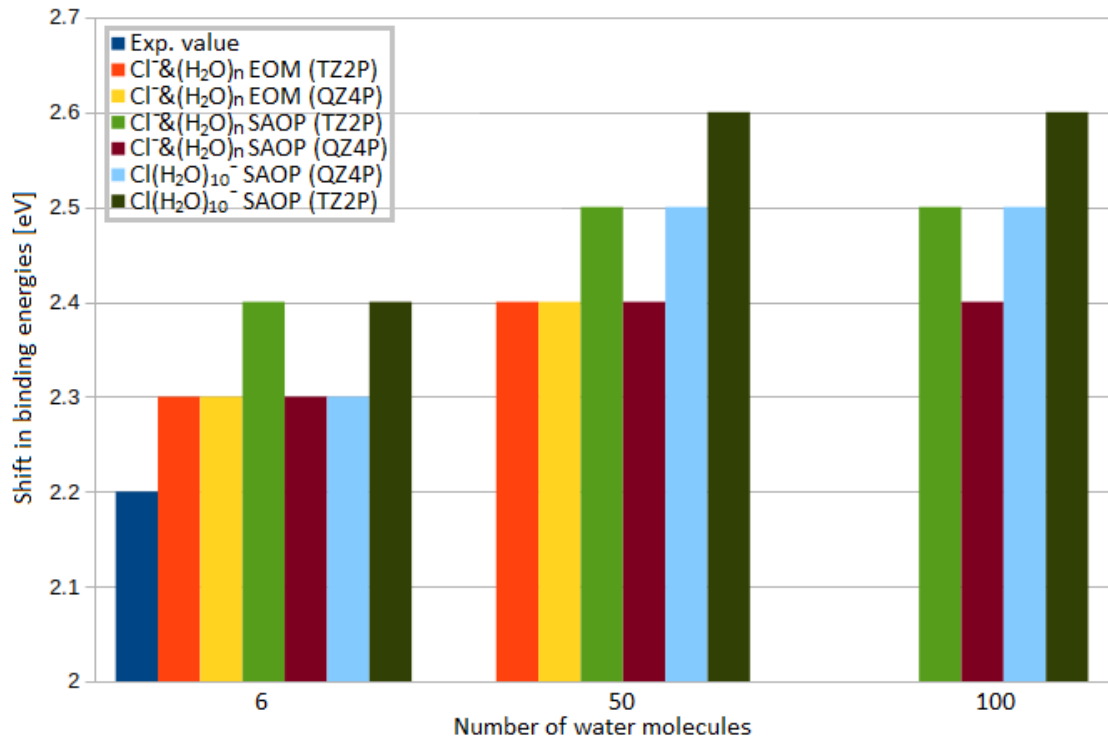
for various water cluster size obtained with DC-ZORA SAOP using QZ4P (figure 1.7 (a), (b), (c) and (f)) and with DC CVS-EOM-IP-CCSD (figure 1.7 (d) and (e)) using TZ2P

**Table 1.1:** Average binding energies (in eV) for the spin-orbit coupling effect of the P states of embedded chloride ion on different water cluster size with DC-ZORA SAOP and DC CVS-EOM-IP-CCSD calculations using triple-zeta basis sets

	$Cl^{-}(2P_{\frac{3}{2}})$ SAOP	$Cl^{-}(2P_{\frac{1}{2}})$ SAOP	Chemical shift 2P states	$Cl^{-}(2P_{\frac{3}{2}})$ EOM	$Cl^{-}(2P_{\frac{1}{2}})$ EOM	Chemical shift 2P states	Ice (1b <sub>1</sub> ) VBM	Ice (3a <sub>1</sub> ) VBM
$Cl^{-1}/(H_2O)_6$	3.4	5.8	2.4(0.08)	3.7	6.0	2.3(0.04)	11.4(0.08)	13.4(0.06)
$Cl^{-1}/(H_2O)_{50}$	3.7	6.2	2.5(0.12)	3.9	6.3	2.4(0.08)	11.5(0.07)	13.5(0.05)
$Cl^{-1}/(H_2O)_{100}$	3.9	6.4	2.5(0.12)				11.6(0.06)	13.6(0.04)
$(Cl(H_2O)_{10})^{-1}/(H_2O)_{40}$	3.8	6.4	2.6(0.15)				11.4(0.08)	13.4(0.06)
$(Cl(H_2O)_{10})^{-1}/(H_2O)_{90}$	4.0	6.6	2.6(0.15)				11.5(0.07)	13.5(0.05)

Table 1.2: Average binding energies (in eV) for the spin-orbit coupling effect of the P states of embedded chloride ion on different water cluster size with DC-ZORA SAOP and DC CVS-EOM-IP-CCSD calculations using quadruple-zeta basis sets

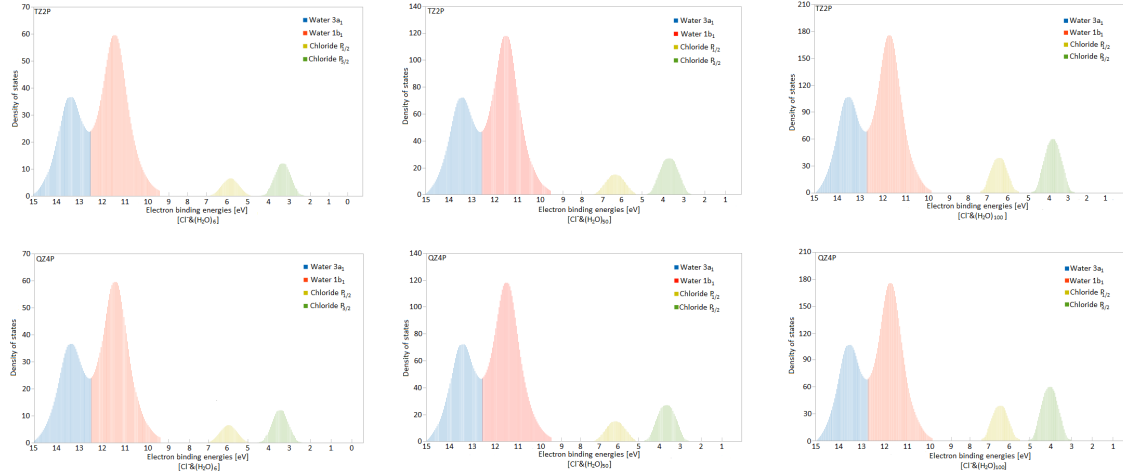
	$Cl^- (2P_{\frac{1}{2}})$ SAOP	$Cl^- (2P_{\frac{1}{2}})$ SAOP	Chemical shift 2P states	$Cl^- (2P_{\frac{3}{2}})$ EOM	$Cl^- (2P_{\frac{1}{2}})$ EOM	Chemical shift 2P states	Ice (1b <sub>1</sub> ) VBM	Ice (3a <sub>1</sub> ) VBM
$Cl^{-1}/(H_2O)_6$	3.6	5.9	2.3(0.04)	3.8	6.1	2.3(0.04)	11.4(0.08)	13.4(0.06)
$Cl^{-1}/(H_2O)_{50}$	3.8	6.2	2.4(0.08)	4.0	6.4	2.4(0.08)	11.5(0.07)	13.5(0.05)
$Cl^{-1}/(H_2O)_{100}$	4.0	6.4	2.4(0.08)				11.6(0.06)	13.6(0.04)
$(Cl(H_2O)_{10})^{-1}/(H_2O)_{40}$	3.9	6.4	2.5(0.12)				11.4(0.08)	13.4(0.06)
$(Cl(H_2O)_{10})^{-1}/(H_2O)_{90}$	4.1	6.6	2.5(0.12)				11.5(0.07)	13.5(0.05)



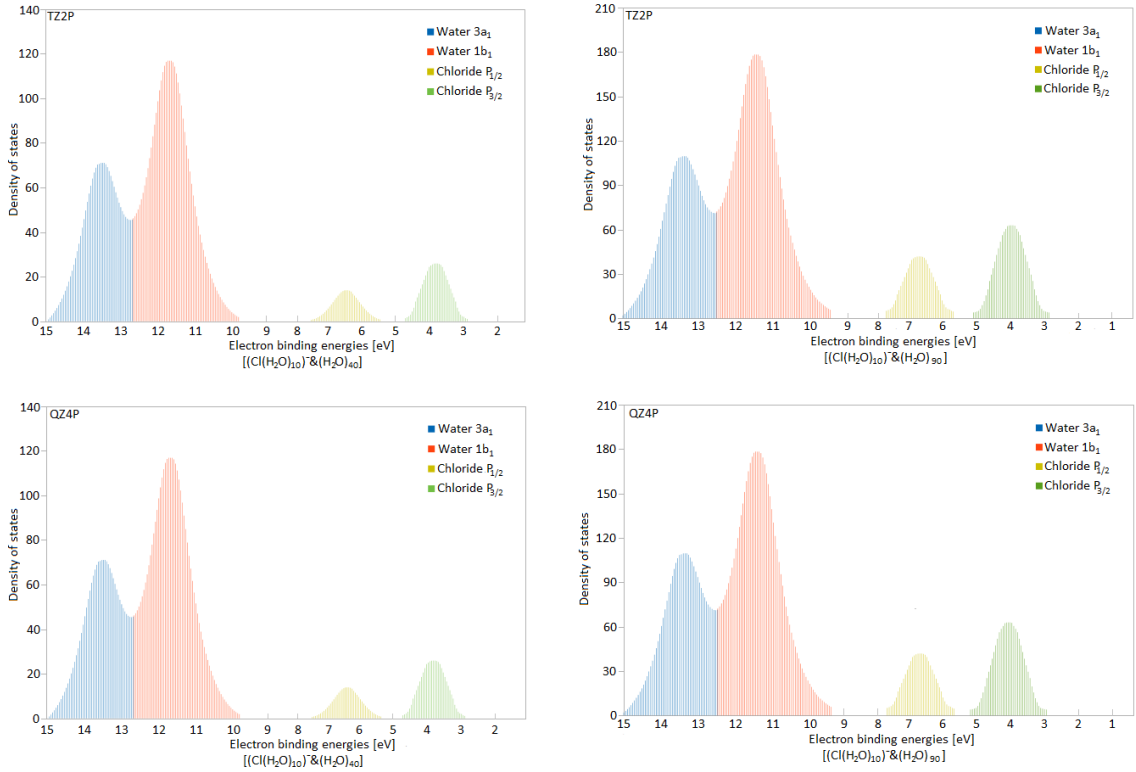
**Figure 1.8:** Computed binding energies shift (in eV) for the spin-orbit coupling effect of the P states of chloride ion embedded in different water cluster size with DC-ZORA SAOP and DC CVS-EOM-IP-CCSD using different basis sets and comparison with experimental value

Table 1.3: Experimental binding energies (in eV) for the valence band maximum (VBM) of ice from (a) (Henderson, 2002), partially solvated chloride ion in pure liquid from (c) (Markovich et al., 1994) and chemical shift for the spin-orbit coupling component of the 2P state of chloride ion on ice surface from (d) (Kong et al., 2017) and (e) (Parent et al., 2011)

	Solvated chloride anion (Pure liquid)	VBM $1b_1$	VBM $3a_1$	Chemical shift 2P state
Ice		12.3 (a)	14.2 (a)	
$Cl^{-1}/ice$				2.2 (d) 1.3 (e)
$Cl^{-1}/(H_2O)_4$	5.92 (c)			
$Cl^{-1}/(H_2O)_5$	6.21 (c)			
$Cl^{-1}/(H_2O)_6$	6.58 (c)			



**Figure 1.9:** Average electron binding energies spectra (in eV) for  $[Cl^{-1}/(H_2O)_n]$  for various water cluster size obtained with DC-ZORA SAOP using TZ2P and QZ4P basis sets



**Figure 1.10:** Average electron binding energies spectra (in eV) for  $[(Cl(H_2O)_{10})^{-1} / (H_2O)_n]$  for various water cluster size obtained with DC-ZORA SAOP using TZ2P and QZ4P basis sets

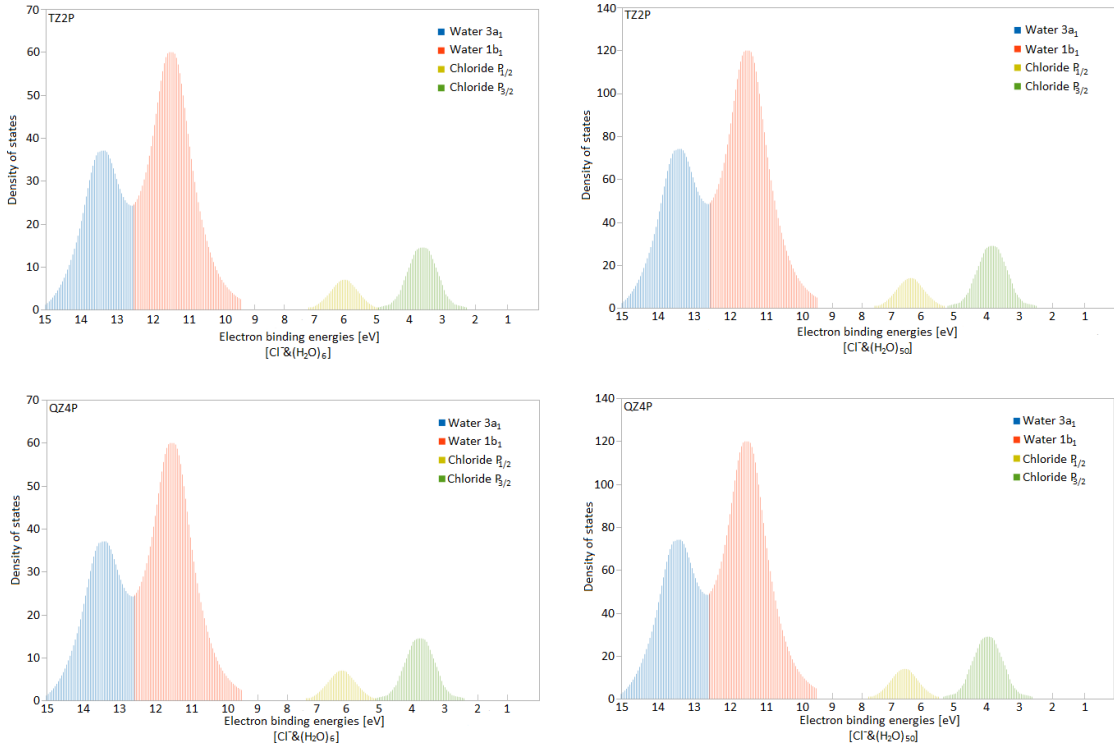


**Figure 1.11:** Average electron binding energies spectra (in eV) for  $[Cl^{-1} / (H_2O)_n]$  for various water cluster size obtained with DC CVS-EOM-IP-CCSD using TZ2P and QZ4P

## 1.6 Results of the impact of Cl ion on ice surface

Density of state (DOS) is useful to investigate the differences in the dynamics of the same kind of molecules. Figure 1.13 (a) and (b) depicts the DOS of chloride ion and solvated chloride ion respectively. The band close to -0.12 au (-3.3 eV) on both figures corresponds to the HOMO of the chloride ion. It can be seen that there is clear difference between the two spectrum. For the solvated chloride ion, the peaks seem to become broader compared to that of the unsolvated chloride ion. This is an indication that the quasi-liquid layer (QLL) on ice surface influences the ionic chloride. We must say that the total DOS changes drastically as the number of water molecules interacting with ionic chloride increases, however, the HOMO energies seem to remain almost the same. This is an indication that only few water molecules on ice surface is required to perturb the chloride and bind them into solvation. Thus, increase in the number of water molceules does lead to significant changes in the the orbital energies of HCl adsorption on ice surface as shown in figure 1.13 and

1.13

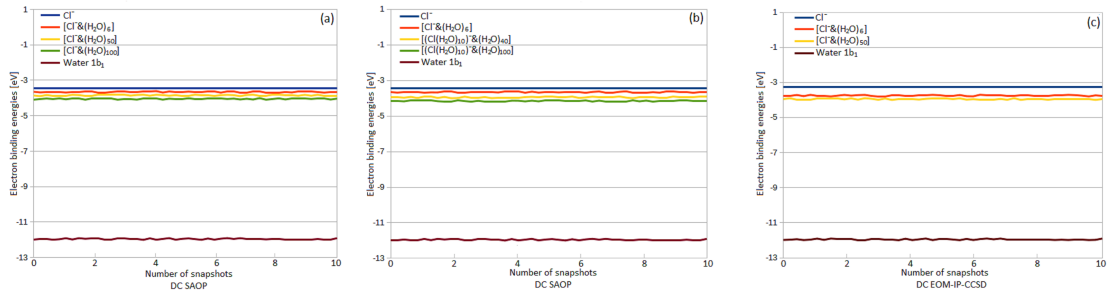


**Figure 1.12:** Impact of the number of water molecules on gas phase chloride ion using DC SAOP with QZ4P (figure 1.12 (a), (b)) in the DFT-in-DFT and DC CVS-EOM-IP-CCSD with TZ2P (figure 1.12 (c)) in the CC-in-DFT approach for 10 snapshots with respect to the binding energies in eV

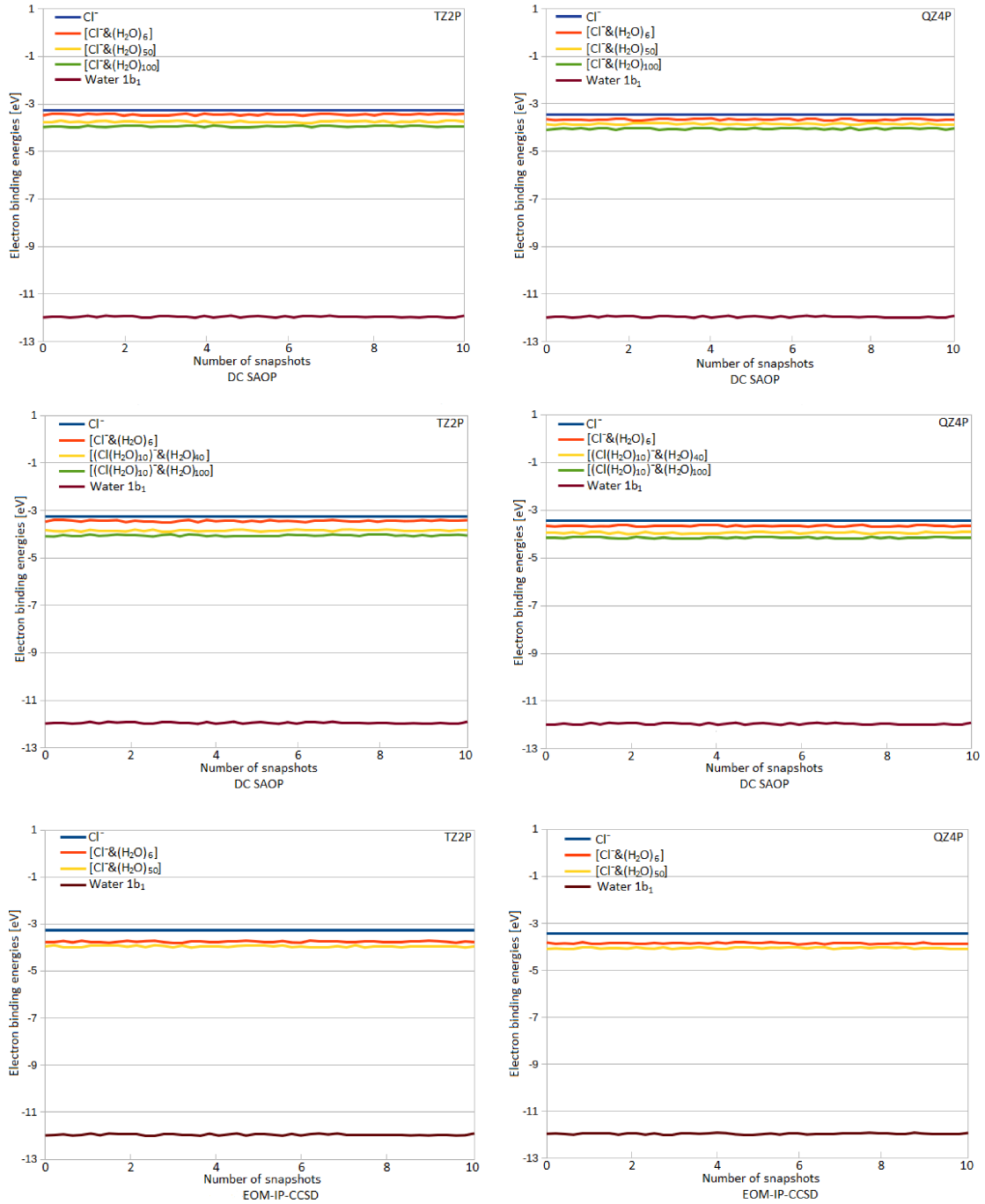


**Figure 1.13:** Impact of the number of water molecules on gas phase chloride ion using DC SAOP in the DFT-in-DFT and DC CVS-EOM-IP-CCSD in the CC-in-DFT approach with different basis sets for 10 snapshots with respect to the binding energies in eV

# References

- Abbatt, J. P. (2003). Interactions of atmospheric trace gases with ice surfaces: Adsorption and reaction. *Chemical reviews*, 103(12):4783–4800.
- Arillo-Flores, O., Ruiz-López, M., and Bernal-Uruchurtu, M. (2007). Can semi-empirical models describe hcl dissociation in water? *Theoretical Chemistry Accounts*, 118(2):425–435.
- Aryasetiawan, F. and Gunnarsson, O. (1998). The gw method.
- Bartels-Rausch, T., Jacobi, H.-W., Kahan, T. F., Thomas, J. L., Thomson, E. S., Abbatt, J. P., Ammann, M., Blackford, J. R., Bluhm, H., Boxe, C., et al. (2014). A review of air–ice chemical and physical interactions (aici): liquids, quasi-liquids, and solids in snow. *Atmospheric chemistry and physics*, 14(3):1587–1633.
- Bartlett, R. J. and Musiał, M. (2007). Coupled-cluster theory in quantum chemistry. *Reviews of Modern Physics*, 79(1):291.
- Blase, X., Boulanger, P., Bruneval, F., Fernandez-Serra, M., and Duchemin, I. (2016). Erratum:“gw and bethe-salpeter study of small water clusters”[j. chem. phys. 144, 034109 (2016)]. *The Journal of chemical physics*, 145(16):169901.
- Bouchafra, Y., Shee, A., Réal, F., Vallet, V., and Gomes, A. S. P. (2018). Predictive simulations of ionization energies of solvated halide ions with relativistic embedded equation of motion coupled cluster theory. *Physical review letters*, 121(26):266001.
- Cederbaum, L. S., Domcke, W., and Schirmer, J. (1980). Many-body theory of core holes. *Physical Review A*, 22(1):206.

Daday, C., Konig, C., Valsson, O., Neugebauer, J., and Filippi, C. (2013). State-specific embedding potentials for excitation-energy calculations. *Journal of chemical theory and computation*, 9(5):2355–2367.

Darvas, M., Lasne, J., Laffon, C., Parent, P., Picaud, S., and Jedlovszky, P. (2012). Adsorption of acetaldehyde on ice as seen from computer simulation and infrared spectroscopy measurements. *Langmuir*, 28(9):4198–4207.

Dau, P. D., Su, J., Liu, H.-T., Liu, J.-B., Huang, D.-L., Li, J., and Wang, L.-S. (2012). Observation and investigation of the uranyl tetrafluoride dianion ( $\text{uo}_2\text{f}_4^{2-}$ ) and its solvation complexes with water and acetonitrile. *Chemical Science*, 3(4):1137–1146.

Dutta, A. K., Vaval, N., and Pal, S. (2018). Lower scaling approximation to eom-ccsd: A critical assessment of the ionization problem. *International Journal of Quantum Chemistry*, 118(14):e25594.

Dutta, A. K., Vavala, N., and Pal, S. (2017). Assessment of low scaling approximations to eom-ccsd method for ionization potential. *arXiv preprint arXiv:1708.01293*.

Dyall, K. G. (2016). Relativistic double-zeta, triple-zeta, and quadruple-zeta basis sets for the light elements h–ar. *Theoretical Chemistry Accounts*, 135(5):128.

Gaiduk, A. P., Govoni, M., Seidel, R., Skone, J. H., Winter, B., and Galli, G. (2016). Photoelectron spectra of aqueous solutions from first principles. *Journal of the American Chemical Society*, 138(22):6912–6915.

Gaiduk, A. P., Pham, T. A., Govoni, M., Paesani, F., and Galli, G. (2018). Electron affinity of liquid water. *Nature communications*, 9(1):247.

Gomes, A. S. P., Jacob, C. R., and Visscher, L. (2008). Calculation of local excitations in large systems by embedding wave-function theory in density-functional theory. *Physical Chemistry Chemical Physics*, 10(35):5353–5362.

- Gordon, B. P., Moore, F. G., Scatena, L. F., Valley, N. A., Wren, S. N., and Richmond, G. L. (2018). Model behavior: Characterization of hydroxyacetone at the air–water interface using experimental and computational vibrational sum frequency spectroscopy. *The Journal of Physical Chemistry A*, 122(15):3837–3849.
- Henderson, M. A. (2002). The interaction of water with solid surfaces: fundamental aspects revisited. *Surface Science Reports*, 46(1-8):1–308.
- Höfener, S., Gomes, A. S. P., and Visscher, L. (2013). Solvatochromic shifts from coupled-cluster theory embedded in density functional theory. *The Journal of chemical physics*, 139(10):104106.
- Höfener, S. and Visscher, L. (2012). Calculation of electronic excitations using wave-function in wave-function frozen-density embedding. *The Journal of chemical physics*, 137(20):204120.
- Hüfner, S. (2013). *Photoelectron spectroscopy: principles and applications*. Springer Science & Business Media.
- Jorgensen, W. L., Chandrasekhar, J., Madura, J. D., Impey, R. W., and Klein, M. L. (1983). Comparison of simple potential functions for simulating liquid water. *The Journal of chemical physics*, 79(2):926–935.
- Kong, X., Waldner, A., Orlando, F., Artiglia, L., Huthwelker, T., Ammann, M., and Bartels-Rausch, T. (2017). Coexistence of physisorbed and solvated hcl at warm ice surfaces. *The journal of physical chemistry letters*, 8(19):4757–4762.
- Kroes, G. J. and Clary, D. C. (1992). Sticking of hydrogen chloride and chlorine hydroxide to ice: A computational study. *The Journal of Physical Chemistry*, 96(17):7079–7088.
- Krepelova, A., Bartels-Rausch, T., Brown, M. A., Bluhm, H., and Ammann, M. (2013). Adsorption of acetic acid on ice studied by ambient-pressure xps and partial-electron-yield nexafs spectroscopy at 230–240 k. *The Journal of Physical Chemistry A*, 117(2):401–409.

Lange, M. F. and Berkelbach, T. C. (2018). On the relation between equation-of-motion coupled-cluster theory and the gw approximation. *Journal of chemical theory and computation*, 14(8):4224–4236.

Lemierre, V., Chrostowska, A., Dargelos, A., and Chermette, H. (2005). Calculation of ionization potentials of small molecules: A comparative study of different methods. *The Journal of Physical Chemistry A*, 109(37):8348–8355.

Lenthe, E. v., Baerends, E.-J., and Snijders, J. G. (1993). Relativistic regular two-component hamiltonians. *The Journal of chemical physics*, 99(6):4597–4610.

Markovich, G., Pollack, S., Giniger, R., and Cheshnovsky, O. (1994). Photoelectron spectroscopy of cl-, br-, and i- solvated in water clusters. *The Journal of chemical physics*, 101(11):9344–9353.

Musiał, M., Perera, A., and Bartlett, R. J. (2011). Multireference coupled-cluster theory: The easy way. *The Journal of chemical physics*, 134(11):114108.

Newberg, J. T. and Bluhm, H. (2015). Adsorption of 2-propanol on ice probed by ambient pressure x-ray photoelectron spectroscopy. *Physical Chemistry Chemical Physics*, 17(36):23554–23558.

Newberg, J. T., Starr, D. E., Yamamoto, S., Kaya, S., Kendelewicz, T., Mysak, E. R., Porsgaard, S., Salmeron, M. B., Brown Jr, G. E., Nilsson, A., et al. (2011). Formation of hydroxyl and water layers on mgo films studied with ambient pressure xps. *Surface Science*, 605(1-2):89–94.

Olivieri, G., Goel, A., Kleibert, A., Cvetko, D., and Brown, M. A. (2016). Quantitative ionization energies and work functions of aqueous solutions. *Physical Chemistry Chemical Physics*, 18(42):29506–29515.

Opalka, D., Pham, T. A., Sprik, M., and Galli, G. (2014). The ionization potential of aqueous hydroxide computed using many-body perturbation theory. *The Journal of chemical physics*, 141(3):034501.

- Parent, P., Lasne, J., Marcotte, G., and Laffon, C. (2011). Hcl adsorption on ice at low temperature: a combined x-ray absorption, photoemission and infrared study. *Physical Chemistry Chemical Physics*, 13(15):7142–7148.
- Peng, B., Lestrage, P. J., Goings, J. J., Caricato, M., and Li, X. (2015). Energy-specific equation-of-motion coupled-cluster methods for high-energy excited states: Application to k-edge x-ray absorption spectroscopy. *Journal of chemical theory and computation*, 11(9):4146–4153.
- Perdew, J. P., Burke, K., and Ernzerhof, M. (1996). Generalized gradient approximation made simple. *Physical review letters*, 77(18):3865.
- Pham, T. A., Govoni, M., Seidel, R., Bradforth, S. E., Schwegler, E., and Galli, G. (2017). Electronic structure of aqueous solutions: Bridging the gap between theory and experiments. *Science advances*, 3(6):e1603210.
- Schipper, P., Gritsenko, O., Van Gisbergen, S., and Baerends, E. (2000). Molecular calculations of excitation energies and (hyper) polarizabilities with a statistical average of orbital model exchange-correlation potentials. *The Journal of Chemical Physics*, 112(3):1344–1352.
- Segala, M. and Chong, D. P. (2009). An evaluation of exchange-correlation functionals for the calculations of the ionization energies for atoms and molecules. *Journal of Electron Spectroscopy and Related Phenomena*, 171(1-3):18–23.
- Shee, A., Saue, T., Visscher, L., and Severo Pereira Gomes, A. (2018). Equation-of-motion coupled-cluster theory based on the 4-component dirac–coulomb (–gaunt) hamiltonian. energies for single electron detachment, attachment, and electronically excited states. *The Journal of chemical physics*, 149(17):174113.
- Shibaguchi, T., Onuki, H., and Onaka, R. (1977). Electronic structures of water and ice. *Journal of the Physical Society of Japan*, 42(1):152–158.
- Solomon, S. (1999). Stratospheric ozone depletion: A review of concepts and history. *Reviews of Geophysics*, 37(3):275–316.

- Starr, D., Pan, D., Newberg, J., Ammann, M., Wang, E., Michaelides, A., and Bluhm, H. (2011). Acetone adsorption on ice investigated by x-ray spectroscopy and density functional theory. *Physical Chemistry Chemical Physics*, 13(44):19988–19996.
- Starr, D. E., Favaro, M., Abdi, F. F., Bluhm, H., Crumlin, E. J., and van de Krol, R. (2017). Combined soft and hard x-ray ambient pressure photoelectron spectroscopy studies of semiconductor/electrolyte interfaces. *Journal of Electron Spectroscopy and Related Phenomena*, 221:106–115.
- Su, J., Dau, P. D., Xu, C.-F., Huang, D.-L., Liu, H.-T., Wei, F., Wang, L.-S., and Li, J. (2013). A joint photoelectron spectroscopy and theoretical study on the electronic structure of ucl5- and ucl5. *Chemistry—An Asian Journal*, 8(10):2489–2496.
- Takahata, Y. and Chong, D. P. (2003). Dft calculation of core-electron binding energies. *Journal of electron spectroscopy and related phenomena*, 133(1-3):69–76.
- Tecmer, P., Gomes, A. S. P., Ekström, U., and Visscher, L. (2011). Electronic spectroscopy of uo<sub>2</sub> 2+, nuo+ and nun: an evaluation of time-dependent density functional theory for actinides. *Physical Chemistry Chemical Physics*, 13(13):6249–6259.
- Tissot, H., Olivieri, G., Gallet, J.-J., Bournel, F., Silly, M. G., Sirotti, F., and Rochet, F. (2015). Cation depth-distribution at alkali halide aqueous solution surfaces. *The Journal of Physical Chemistry C*, 119(17):9253–9259.
- Toubin, C., Picaud, S., Hoang, P., Girardet, C., Demirdjian, B., Ferry, D., and Suzanne, J. (2001). Dynamics of ice layers deposited on mgo (001): Quasielastic neutron scattering experiments and molecular dynamics simulations. *The Journal of Chemical Physics*, 114(14):6371–6381.
- Van Lenthe, E. and Baerends, E. J. (2003). Optimized slater-type basis sets for the elements 1–118. *Journal of computational chemistry*, 24(9):1142–1156.
- Wick, C. D. (2017). A comparison of sodium and hydrogen halides at the air-water interface. *The Journal of chemical physics*, 147(16):161703.

- Woittequand, S., Duflot, D., Monnerville, M., Pouilly, B., Toubin, C., Briquez, S., and Meyer, H.-D. (2007). Classical and quantum studies of the photodissociation of a hx (x= cl, f) molecule adsorbed on ice. *The Journal of chemical physics*, 127(16):164717.
- Yamamoto, S., Kendelewicz, T., Newberg, J. T., Ketteler, G., Starr, D. E., Mysak, E. R., Andersson, K. J., Ogasawara, H., Bluhm, H., Salmeron, M., et al. (2010). Water adsorption on  $\alpha$ -fe<sub>2</sub>o<sub>3</sub> (0001) at near ambient conditions. *The Journal of Physical Chemistry C*, 114(5):2256–2266.